







The dynamics of molecular, immune and physiological features of the host and the gut microbiome, and their interactions before and after onset of laying in two hen strains

Siriluck Ponsuksili ^{*,1}, Frieder Hadlich ^{*}, Alvaro Perdomo-Sabogal^{*}, Henry Reyer ^{*}, Michael Oster^{*}, Nares Trakooljul ^{*}, Muhammad Arsalan Iqbal^{*}, Sonja Schmucker ^{†,‡}, Volker Stefanski[†], Christoph Roth[†], Amélia Camarinha Silva[†], Korinna Huber[†], Vera Sommerfeld [†], Markus Rodehutsord[†] and Klaus Wimmers^{*,‡}

^{*}Research Institute for Farm Animal Biology (FBN), Institute for Genome Biology, 18196 Dummerstorf, Germany; [†]University of Hohenheim, Institute of Animal Science, 70599 Stuttgart, Germany; and [‡]University Rostock, Faculty of Agricultural and Environmental Sciences, 18059 Rostock, Germany

ABSTRACT Aggregation of data, including deep sequencing of mRNA and miRNA data in jejunum mucosa, abundance of immune cells, metabolites, or hormones in blood, composition of microbiota in digesta and duodenal mucosa, and production traits collected along the lifespan, provides a comprehensive picture of lifelong adaptation processes. Here, respective data from two laying hen strains (Lohmann Brown-Classic (**LB**) and Lohmann LSL-Classic (**LSL**) collected at 10, 16, 24, 30, and 60 wk of age were analyzed. Data integration revealed strain- and stage-specific biosignatures, including elements indicative of molecular pathways discriminating the

strains. Although the strains performed the same, they differed in the activity of immunological and metabolic functions and pathways and showed specific gut-microbiota-interactions in different production periods. The study shows that both strains employ different strategies to acquire and maintain their capabilities under high performance conditions, especially during the transition phase. Furthermore, the study demonstrates the capacity of such integrative analyses to elucidate molecular pathways that reflect functional biodiversity. The bioinformatic reduction of the multidimensional data provides good guidance for further manual review of the data.

Key words: Multi-omics, RNAseq, laying hen, immune cells, host-gut microbiota

2023 Poultry Science 102:102256

<https://doi.org/10.1016/j.psj.2022.102256>

INTRODUCTION

Metabolic and mineral requirements change throughout life in parallel with maturation, growth, and egg production, especially from chick to sexual maturity in pullets (~18 wk) to the onset of laying (~24 wk), as egg production increases (~30 wk) until gradually decreasing laying performance (~60 wk). During these developmental phases, a dynamic balance occurs between the changing endogenous requirements and the exogenous factors, to which changes in the microbiota of the host intestinal tract also contribute. Knowledge of the molecular drivers that are causal for the physiological and metabolic adaptations provides clear insights into the ontogeny throughout the life cycle of laying hens.

Systems biology helps to decipher the complex biology for changes during the life span of laying hens, and eventually reveal interactions between key features.

Phosphorus (**P**) and calcium (**Ca**) are essential nutrients in particular for laying hens to fulfill their laying performance. The small intestine is the main site of nutrient uptake including P and Ca. Mineral P is a limited resource globally but highly bioavailable to monogastrics, whereas P contained in plant seeds in form of inositol phosphates (**InsPx**) cannot be efficiently utilized by monogastrics due to the lack or scarcity of an endogenous phytases. In poultry, the extent of phytate (**InsP₆**) degradation was found to be incomplete and highly variable (Rodehutsord, 2017). Different gut microbes are capable to exert phytase and phosphatase activities affecting the availability of plant-derived P, but in turn the gastrointestinal microbial community is influenced by dietary supplementation with Ca, P, or phytase (Borda-Molina et al., 2016).

The host's gut microbiota ecosystem is a gateway to the host organism and is constantly exposed to feed components and foreign antigens. Changes in various aspects of

© 2022 The Authors. Published by Elsevier Inc. on behalf of Poultry Science Association Inc. This is an open access article under the CC BY-NC-ND license (<http://creativecommons.org/licenses/by-nc-nd/4.0/>).

Received July 22, 2022.

Accepted October 11, 2022.

¹Corresponding author: ponsuksili@fbn-dummerstorf.de

host physiology related to metabolism, immune defense, energy allocation, and health status are influenced by the gut microbiota (Barko et al., 2018). Conversely, the microbiota is dynamic and changes according to the age, nutrition, and health status of the host (Ottman et al., 2012; Heimritz et al., 2016).

In our previous studies, animals of 2 laying hen strains (Lohmann Brown-Classic [LB], Lohmann LSL-Classic [LSL]) were studied over 5 developmental stages. These studies focused on individual data sets at various biological levels, such as physiological, endocrine, metabolic, immune, and transcriptomic (Sommerfeld et al., 2020a; Gonzalez-Uarquin et al., 2021; Omotoso et al., 2021; Ponsuksili et al., 2021; Schmucker et al., 2021). All data sets were obtained with the same animals. Although the LB and LSL strains have been selected for egg production (<http://www.ltz.de/en/layers/>), achieving approximately identical performances, they have also been extensively monitored to ensure high standards of bone mineralization, egg quality, and animal welfare (Kaufmann et al., 2011; Habig et al., 2012). However, it is evident that the LB and LSL layer strains achieve these performances against a background of significantly different metabolic strategies and resource allocation (Iqbal et al., 2022) related to P, including InsP₆ concentration, phosphatase, phytase, and myo-inositol oxygenase (MIOX) activities in different parts of the gastrointestinal tract (Sommerfeld et al., 2020b). LSL hens showed lower body weight but similar average egg weight compared to LB hens throughout the trial (Sommerfeld et al., 2020b). Strain effects also existed in hormones involved in P and Ca homeostasis, including triiodothyronine, estradiol, calcidiol, and calcitriol (Omotoso et al., 2021). LSL hens seem to have a rather adaptive immunological phenotype, while LB hens have a pronounced innate immunological phenotype (Hofmann et al., 2021). These findings were confirmed at the molecular level of miRNAs and their target transcripts, which show that in LB, miRNA target transcripts were enriched for metabolic pathways, whereas in LSL, miRNA targets were more abundant for immune and inflammatory processes (Ponsuksili et al., 2021). The microbial community differed significantly between strains and gut sections. The marked changes in nutrients, especially Ca, from pre-laying to laying between 16 and 24 wk of age, resulted in the most striking difference not only in metabolic, endocrine, immunological and transcriptomic traits, but also in the gut's microbial community (Sommerfeld et al., 2020b; Gonzalez-Uarquin et al., 2021; Omotoso et al., 2021; Ponsuksili et al., 2021; Schmucker et al., 2021).

Although individual analysis of each dataset for the 2 strains of laying hens across the production period revealed specific differences (Sommerfeld et al., 2020a; Gonzalez-Uarquin et al., 2021; Omotoso et al., 2021; Ponsuksili et al., 2021; Schmucker et al., 2021), a holistic and integrated multi-omics perspective across the lifespan of hens is lacking. The integration of multi-omics analyses may reveal dynamic molecular and physiological changes in host-gut microbiome interactions at different

production periods for the 2 strains of laying hens. Consequently, building on previous studies and datasets, we have compiled a comprehensive systems biology study throughout the entire production period of LB and LSL laying hens. By including deep sequencing of mRNA and miRNA data in jejunum mucosa, the abundances of immune cells, metabolites or hormones in blood, and the microbiota composition in both digesta and duodenal mucosa, we detected longitudinal changes consistent with age- and strain-dependent changes in functional pathways. We also identified biosignatures that may be of relevance for characterizing breed-specific molecular and physiological changes. Finally, host-microbiome interactions and changes in immune and metabolic systems were performed in relation to physiological and performance traits.

MATERIALS AND METHODS

Experimental Procedures, Samplings, and Measurements

All the data for the research presented here originated from several recently published works (Sommerfeld et al., 2020a; Gonzalez-Uarquin et al., 2021; Omotoso et al., 2021; Ponsuksili et al., 2021). In order to supplement the understanding of these current findings and to help this manuscript stand alone, a brief detail of the experiment is described. All animal used in the experiment was conducted in accordance with the German Animal Welfare Legislation approved by the Regierungspräsidium Tübingen (approval number HOH50/17TE). The animal experiment was performed in a 2 × 5 factorial arrangement with laying hen strain and stage of production as factors as detailed in Sommerfeld et al. (2020a). A total of 100 laying hens of the strains Lohmann LSL-Classic (LSL) and Lohmann Brown-Classic (LB) were used. The hens were fed with a corn-soybean meal-based diet with recommended P and Ca levels. The feed formulations covered starter, grower, pre-laying (PL), and laying diets. The feed was formulated to minimize plant-based phytases and contained no exogenous phytases of microbial origin. Birds were sampled at weeks 10, 16, 24, 30, and 60 of life to cover relevant periods of the production cycle, that is, pullets, pre-layer, onset of laying, peak of laying, and senescence. Hens were stunned and subsequently slaughtered by exsanguination at 0900 to 1400 h. Trunk blood or vein blood was collected dependent on the targets of analysis based immune, metabolites, P, Ca, myo-inositol or hormones. Tissue samples for transcriptome profiling were collected from jejunum mucosa, while digesta and mucosa from duodenum were collected for microbiome analysis.

Data Integration

Raw data preprocessing of mRNA and miRNA were previously reported (Omotoso et al., 2021;

Ponsuksili et al., 2021). In brief, after quality control and preprocessing of raw sequencing reads was performed, low-quality reads were removed. The resulting reads were mapped to the chicken genome assembly (GRCg6a, Ensembl release 95). Further, transcripts read counts (mRNA and miRNA) were transformed using a variance-stabilizing transformation method implemented in DESeq2 and used as input for further analysis (Love et al., 2014). Immune data from the same birds were collected (Schmucker et al., 2021), counts of immune cells in the blood, spleen, and cecal tonsil were log₂ transformed. Metabolome data (Gonzalez-Uarquin et al., 2021) were normalized by logarithmic transformation, mean-centered, and divided by the square root of the standard deviation of each variable (Pareto scaling) using MetaboAnalyst 4.0 (Chong et al., 2018). Microbiota data was represented as amplicon sequence variant (ASV) that was deduced from 16S rRNA sequencing from the duodenal mucosa and the duodenal digesta of LB and LSL. Initially, ASVs were assigned to taxa at the genus level and were filtered so that only taxa with more than one observation in at least half of the samples were considered. The normalized ASV abundances of microbiota were further transformed using a variance-stabilizing transformation method implemented in DESeq2 and used as input for further analysis (Love et al., 2014). Other phenotypic traits such as body weight, feed intake, Ca, and P traits from a previous study of the same animals were used as raw data (Sommerfeld et al., 2020a).

In order to generate predictive models to identify biosignatures along the lifespan, between age and strain, and focusing particularly on strain-specific features in the transition period based on the 6 datasets of biological categories, we used the supervised framework for multi-block sPLS discriminant analysis (sPLS-DA). This Data Integration framework for Analysis and Biomarker discovery (DIABLO, available in the R package ‘mixOmics’ (version 6.17.1)) (Rohart et al., 2017; Singh et al., 2019b) uses Latent components, linear combinations of associated latent variables.

DIABLO can be used to integrate complex data sets of heterogeneous origin generated by different platforms and measured on different scales. To evaluate the number of parameters, global performance, balanced error rate (BER), select the optimal metric distance, and determine the number of components for our block.splsda analysis, we used the evaluation function perf() from DIABLO. As input arguments we used the block.splsda object, Mfold validation (folds = 10), repeated the cross-validation (50 repetitions). We fine-tuned our model using tune.block.splsda() function, and determined the optimal number of variables kept for our final block.splsda analysis and downstream analysis. The output from the evaluation step perf() was used to perform the M-fold cross-validation within the tune.block.splsda() step. We used the centroid distance, as our tune.block.splsda() results suggested it produced the best accuracy estimates. The overall balanced error rate (BER) was used to determine the optimal number of

components. In our case, 2 or 3 components were used depending on the comparison group, which can reduce the balanced error rate (BER) < 0.2.

We then applied the mixomics block.splsda() function using our data as input, and the features to select from each component. The discriminant analysis results were visualized by circosplot() functions. While using circosplot() function, we applied a coefficient score (r = 0.8) over components.

Gene ontology and KEGG pathway enrichment analyses were performed for a full set of gut mRNAs correlated with biosignature immune cells and microbiota at cutoff criteria of $P \leq 0.01$ and $r \geq \pm 0.6$ for LB and LSL separately. These correlated mRNAs were subjected to gene ontology enrichment analysis using DAVID (version.6.8), while pathway enrichment analysis using ClueGO generated the KEGG pathway enrichment networks (Bindea et al., 2009; Bindea et al., 2013).

RESULTS

The integration of different biological datasets revealed changes orchestrated in different tissues, including metabolites and immune cells in blood, mRNA and miRNA transcripts in jejunum mucosa, and microbiota both in duodenum digesta (DD) and mucosa (DM). This integration also highlighted their interaction within the host (Figure 1A). We used 6 datasets including 58 immune traits, 209 microbial taxa, 291 miRNAs, 13689 mRNAs, 11 zootechnical or physiological traits, and 183 metabolites, enzymes, or hormones across five production periods of LB and LSL strains. Our results identify biosignatures in 3 categories: along the lifespan, between age and strain, and finally with a particular focus on strain-specific features in the transitional period at the onset of egg laying (Figure 1A). Therefore, mRNA transcripts that were shown to correlate with strain-specific biosignatures of immune cells and microbes in the transition period were analyzed using DAVID (version 6.8) for Gene Ontology (biological processes) and KEGG pathway enrichment (Figure 1B).

Longitudinal Profile Changes Over the Life Span

For integration, classification, feature selection, and visualization of longitudinal data that change across the lifespan, we used a multiblock discriminant analysis for Omics studies using DIABLO (Data Integration Analysis and Biomarker discovery using Latent variable approaches). DIABLO uses multi-omics integrative methods to identify common information across complex datasets with a small number of samples (Rohart et al., 2017; Singh et al., 2019a). It also enables the selection of subsets of the most discriminant features between the time points without considering strains, over 2 derived components with a balanced error rate (BER) < 0.2. Each block of data including mRNA, miRNA, microbiota, phenotype, immune and metabolome showed the separation between

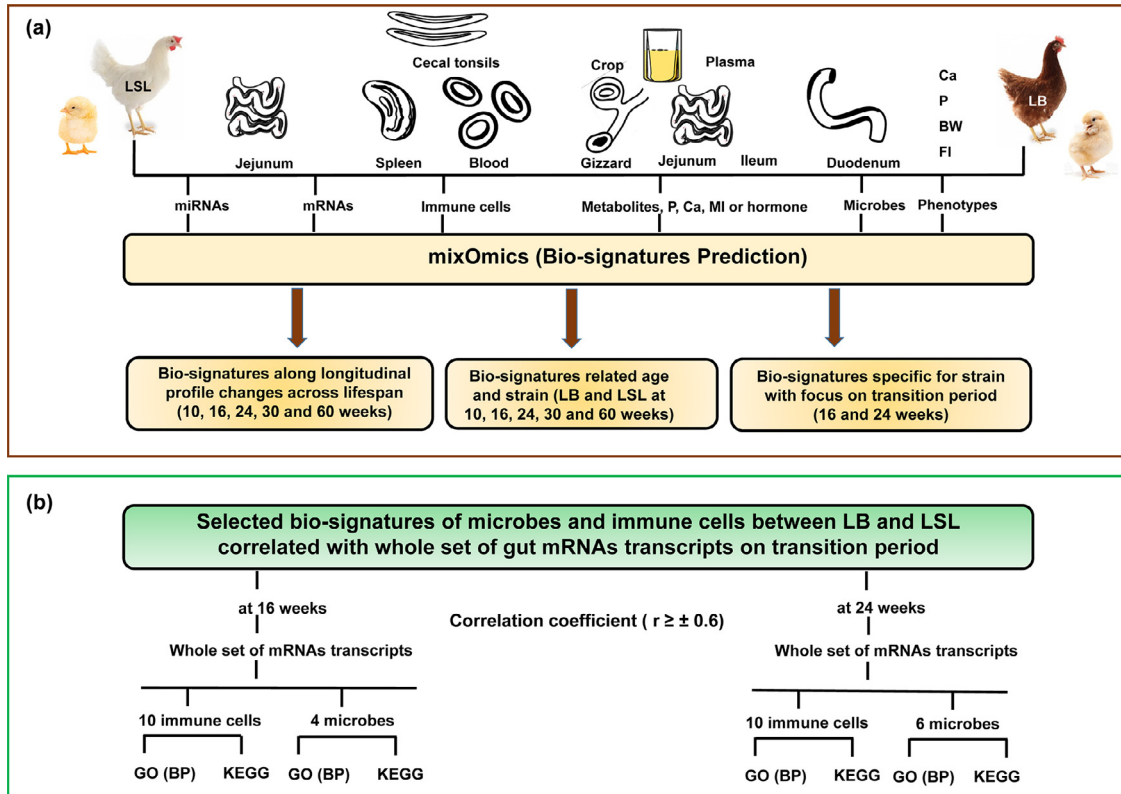


Figure 1. Flowchart of the main steps for biosignature analysis in different groups using mixOmics. (A) The features from different organs, age groups, and strains were used as input. Biosignatures were identified along the hen lifespan, between age and hen strain, and strain-specific in the transition phase to egg laying. (B) Whole gut transcripts correlated with identified specific biosignatures of immune cells and microbes differing between strains in transition period were analyzed using DAVID (version 6.8) for Gene Ontology (biological processes) and KEGG pathway enrichment analysis.

pre- (10 and 16 wk) and post-laying onset (24 and 30 wk). In addition, at 60 wk of age, mRNA and metabolome blocks showed a clearly separation from other time points (Figure 2). In summary 15 mRNAs, 14 miRNAs, 9 microbial taxa, 24 immune traits, 20 metabolites, and 9 phenotypes over 2 component sets were revealed as optimal omics to separate the laying hens age of 10, 16, 24, 30, and 60 wk (Supplementary Table 1). The heat map of the biomarker panel showed 3 major clusters covering the pre-laying period (10 and 16 wk), the onset/peak of laying (24 and 30 wk) and the end of the laying period (60 wk) (Figure 3).

Discriminant features with different abundances before (wk 10, 16) and after onset of laying (wk 24, 30, 60) were found associated with strong metabolic changes. Features being higher abundant at the early stages cover the transcripts *VSIG10*, *PEBP1* and the miRNAs miR181-5p, miR122-5p, miR-1782, miR-184-3p, and let-7d. At later time points (24–60 wk), several key features emerged such as miR-29b-3p, mRNAs including *STARD*, *MSMMO1*, and *HMGCR*, microbes assigned to *Lactococcus*, *Veillonella*, *Fusobacterium*, metabolites represented by phosphatidylcholines, most of the phenotypes and immune cells (thrombocyte, B cell, CD8 T cell in spleen and cecal tonsil). Some clusters showed higher abundance in the range of 10 to 30 wk, with most features belonging to immune cells in blood and spleen. Some clusters showed patterns essentially marked by higher abundance at 24 wk and 30 wk, that

is, due to major changes around the start of laying, contrasting with their levels at wk 60. This pattern belongs to transcripts of mRNA (*PLA2G6*, *NDEL1*, *ENS-GALG0000002389*, *PPARD*, *ST14*, *SLC13A2*, *IRF1*, *AP2B1*, *PAPSS2*, and *SBNO2*) and miRNA (gga-miR-184-3p, gga-miR-130b-3p, gga-miR-21-5p, mmu-miR-6240, mmu-miR-3968, gga-miR-425-5p, gga-miR-2954, and gga-miR-1306-5p). Microbes assigned to *Enhydrobacter* and *Mycoplasma* also appeared prominent at 24 wk while *Brachyspira* and *Alloprevotella* were dominant at 60 wk.

Identification of Biosignatures Related to Age and Strain

Our aim was also to identify biosignatures of key molecular features whose correlated expression is typical for each experimental group and thus reveal an overall distinction and insight into the recruitment of metabolic pathways and endogenous resources. Therefore, we integrated 6 datasets using DIABLO that revealed highly correlated multi-omics signatures to discriminate groups by their genetic background (LB and LSL) and production period (wk 10, 16, 24, 30, 60) over three components with the balanced error rate (BER) <0.2.

All features identified as specific biosignatures of each group are summarized in a circus plot in Figure 4. As detailed in the circos plot these biosignatures selected by

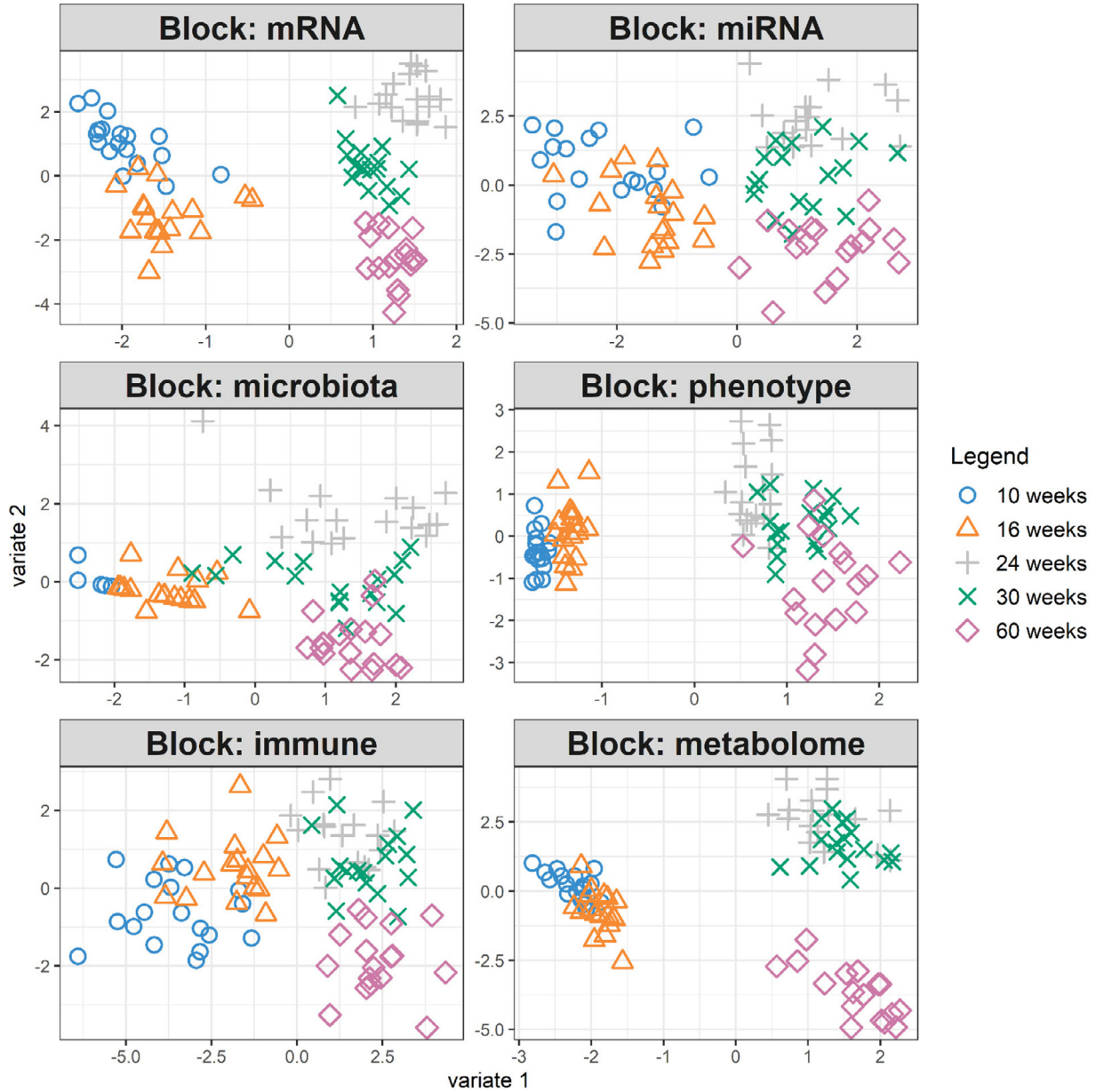


Figure 2. Sample plots for each multi-omics panel depicting a considerable separation between production periods using supervised methods in the R Package mixOmics as the basis for identify key molecular drivers from the panels.

DIABLO consist of 40 mRNAs, 14 miRNAs, 15 microbial taxa, 30 metabolites, 45 immune traits, and 15 other phenotype traits (Supplementary Table 2). Seven out of 40 mRNAs belong to metabolic pathways (gga01100): *AKR1E2*, *HMGCR*, *IVD*, *MSMO1*, *MTHFS*, *PAPSS2*, and *ST6GALNAC1*. The set of 14 selected miRNAs comprises interesting transcripts such as gga-miR-181b-5p and gga-miR-122-5p (Supplementary Table 2). The abundance of *Lactococcus* and *Veillonella* in duodenal mucosa and digesta was determined as biomarkers for different production periods and strains. Plasma metabolites, including phosphatidylcholine, lysophosphatidylcholine, and inositol derivatives in the gut, are also part of the biomarker panels. Many immune cell counts whether they are from spleen (S), cecal tonsils (CT) or blood (B) are part of the bio-signatures. Finally, other phenotype traits including body weight, feed intake and Ca intake as well as P and Ca utilization or excretion

considerably contributed to the distinction of groups. In terms of biosignatures, we found transcripts of *HMGCR*, *MSMO1*, *STARD4*, and *FOCAD* strongly positively correlated with phosphatidylcholine, blood Ca, Ca intake, *Lactococcus*, and body weight ($r > 0.9$; Figure 4). A highly negative correlation was observed between *VSIG10* and miRNA-181b-5p transcripts with phosphatidylcholine, blood calcium, Ca intake, *Lactococcus* and body weight ($r < -0.9$).

Biosignatures Specific to Laying Hens Strain With Focus on the Transition Period

When comparing LB and LSL strains, we focused on 16 and 24 wk as transition period. At 16 wk, a total of 48 features were identified to discriminate between LB and LSL (Supplementary Table 3, Figure 5). For biomarker-

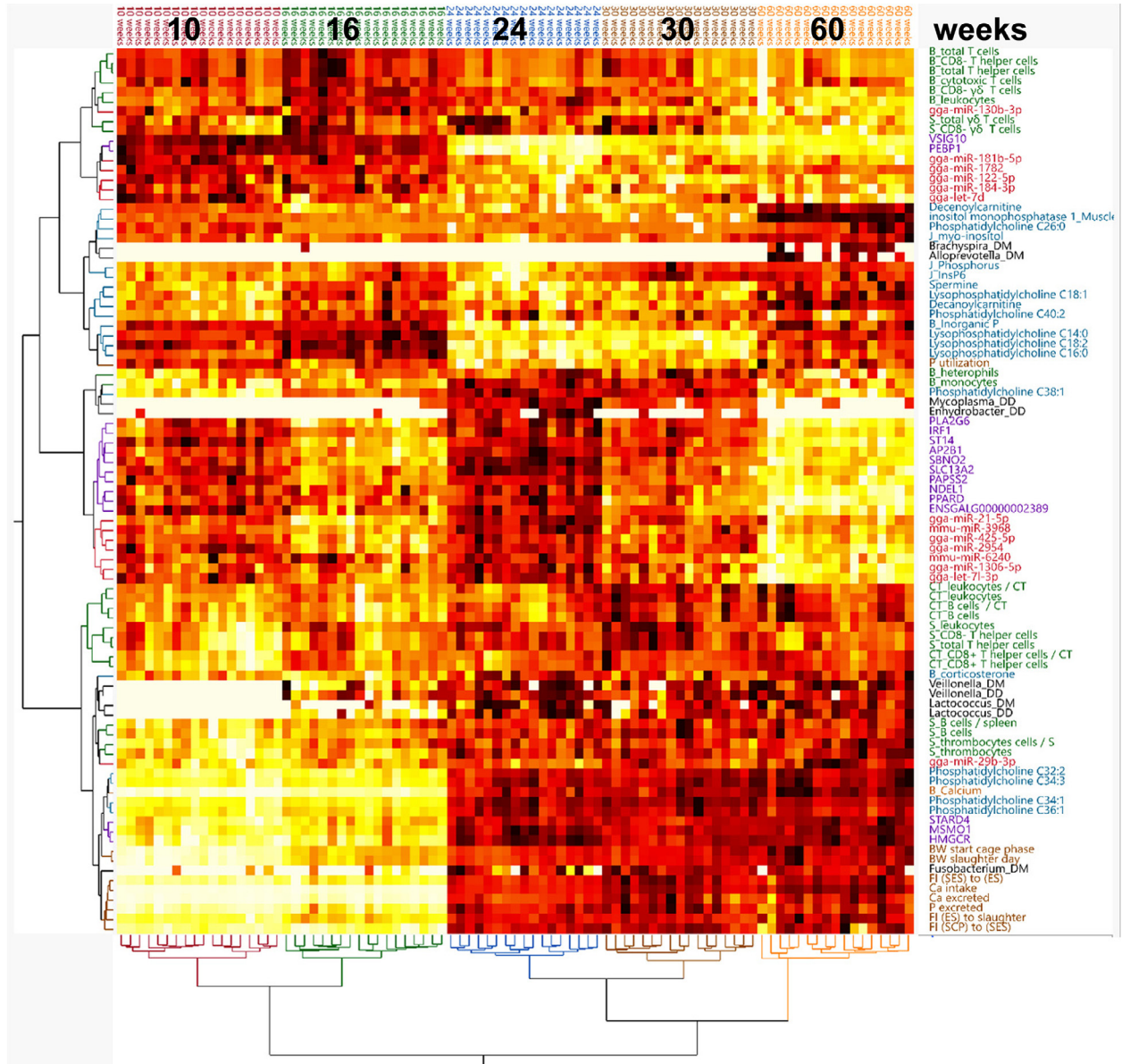


Figure 3. Heatmap of key molecular drivers from multi-omics assays in each production period group. The features cluster into pre-layer (10–16 wk) and layer (24–60 wk) periods. Features were labeled on the left with different colors: red for miRNA, purple for mRNA, green for immune cells, black for microbes, blue for metabolites, and brown for phenotypes.

specific laying hens strain focus on transition period, only 2 latent components are needed to lower the balanced error rate (BER) <0.2. Interestingly, all immune cell counts were higher in LSL than LB at 16 wk. In addition, the *HCK* transcript correlated strongly with CD8- $\gamma\delta$ -T cells, miR-7460-3p, *Terrisporobacter*, and serum serine. *ENSGALG000048571* and brain-specific serine protease (*PRSS22*) correlated negatively with CD8- $\gamma\delta$ T cells, miR-7460-3p, serum serine, and *Terrisporobacter*. We further investigated the functional annotation of gut mRNA transcripts associated with the consistent patterns of discriminating biosignatures of immune cells. We found that the expression levels of 89 to 3,341 transcripts were correlated with the counts of different immune cells (Figure 6A) belonging to biological processes (Figure 6B) and KEGG pathways such as apoptosis signaling, autophagy, immune response, or cytokine-cytokine receptor interaction (Figure 6C).

Moreover, four microbial taxa were identified, including *Catabacter*, *Christensenella*, and *Collinsella*, which were more abundant in the LB strain, while *Terrisporobacter* was more abundant in the LSL strain (Figure 7A). In addition, the relationship between host gut transcripts and the identified microbiota was investigated. Transcripts that correlated with *Terrisporobacter* were enriched in biological processes of response to stimuli or regulation of transport (Figure 7C). The LB enriched transcripts that correlated with the microbiota are related to metabolic pathways, in particular, oxidative phosphorylation, inositol phosphate metabolism, ribosome, and insulin signaling pathways of the KEGG pathways (Figures 7B and 7D).

At 24 wk of age, 87 features revealed differential resource allocation between LB and LSL shortly after the onset of laying (Supplementary Table 4, Figure 8). Positive correlations occur between *HCK*, total T-cell count,

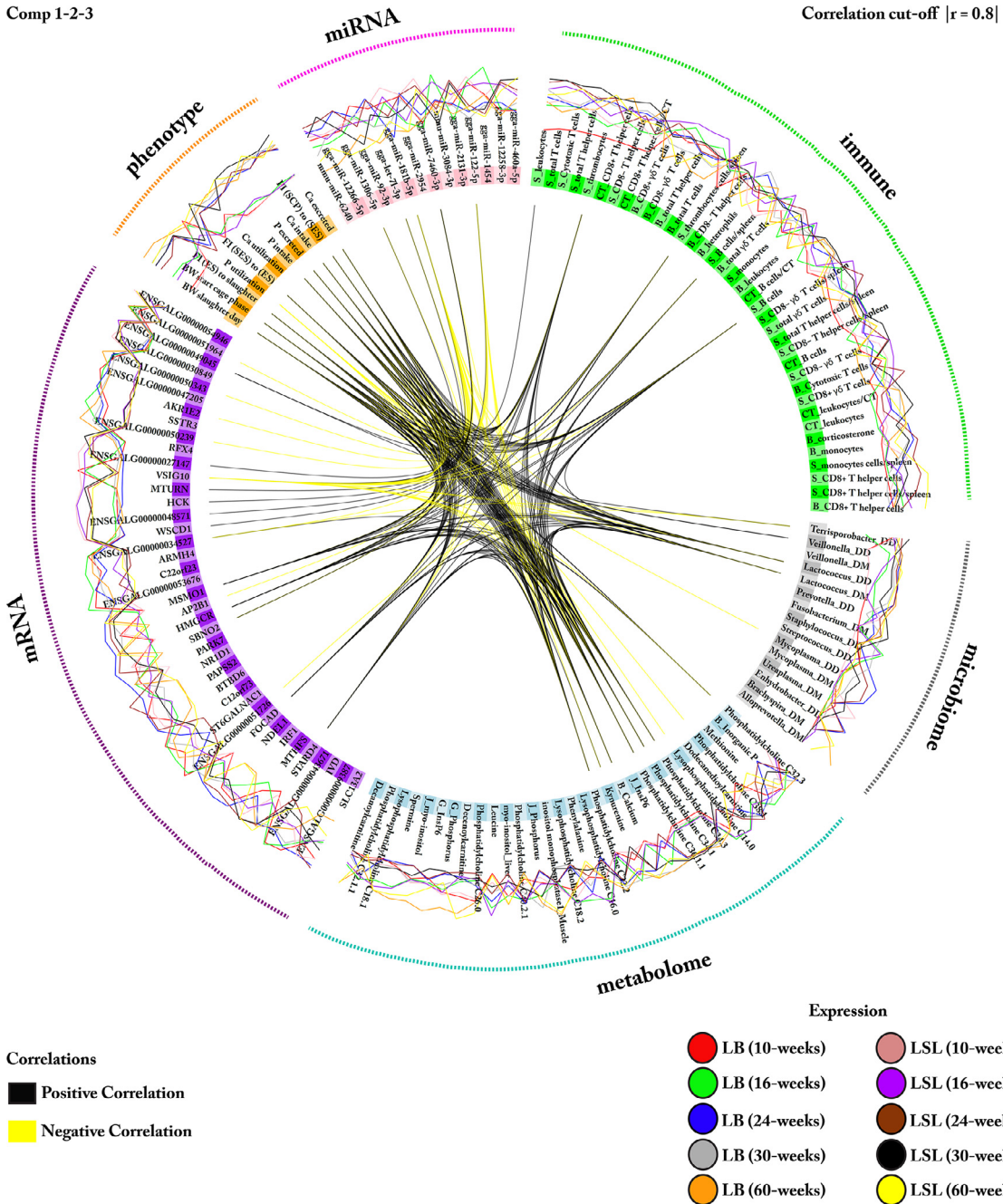


Figure 4. Circos plot displaying the significant biosignatures from multiple blocks over the three components. The selected biomarkers were represented on the side of the circos plot with the block of immune (green), metabolome (blue), mRNA (purple), miRNA (pink), microbiota (gray) and phenotype (orange). Coloured lines in the outer circle indicate expression level in each group. The yellow and black colours within the circle link features and indicate a negative or positive correlation, respectively.

the abundance of *Blautia*, miR-181a-5p and miR-7460-3p, whereas the novel gene ENSGALG00000006083 (Lamin-L(III)-like) was negatively correlated with total T-cell count and *Blautia*. Six out of 10 immune cell types were more abundant in LSL than LB (Figure 9A). The number of intestinal transcripts correlated with the number of immune cells ranged from 131 to 3,251, and these were enriched in at least 15 biological process in LB (Figure 9B) and LSL (Figure 9C) as well as in signaling pathways, including immune system processes (Figure 9D). Out of the 7 microbiota features that were identified, 5 were more abundant in LSL: *Blautia*, *Bacteroides*, *Ruminococcaceae* (unclassified), *Paracoccus*, and

Prevotella. In LB, the *Anaerobiospirillum* and *Enterobacter* microbiota were more abundant (Figure 10A). Most correlated transcripts were found with *Bacteroides* or with *Blautia*. Biological processes and pathways of transcripts correlated with microbes in LB and LSL were shown in Figures 10B–10D. Transcripts negatively correlated with *Bacteroides* or *Blautia* were enriched in the metabolic pathways of oxidative phosphorylation, citrate cycle (TCA cycle), propanoate metabolism, and pyruvate metabolism. For unclassified *Ruminococcaceae*, negatively correlated transcripts were enriched most in proteasome, RNA polymerase, and ribosome. While positively correlated transcripts from *Bacteroides*, *Blautia*, and

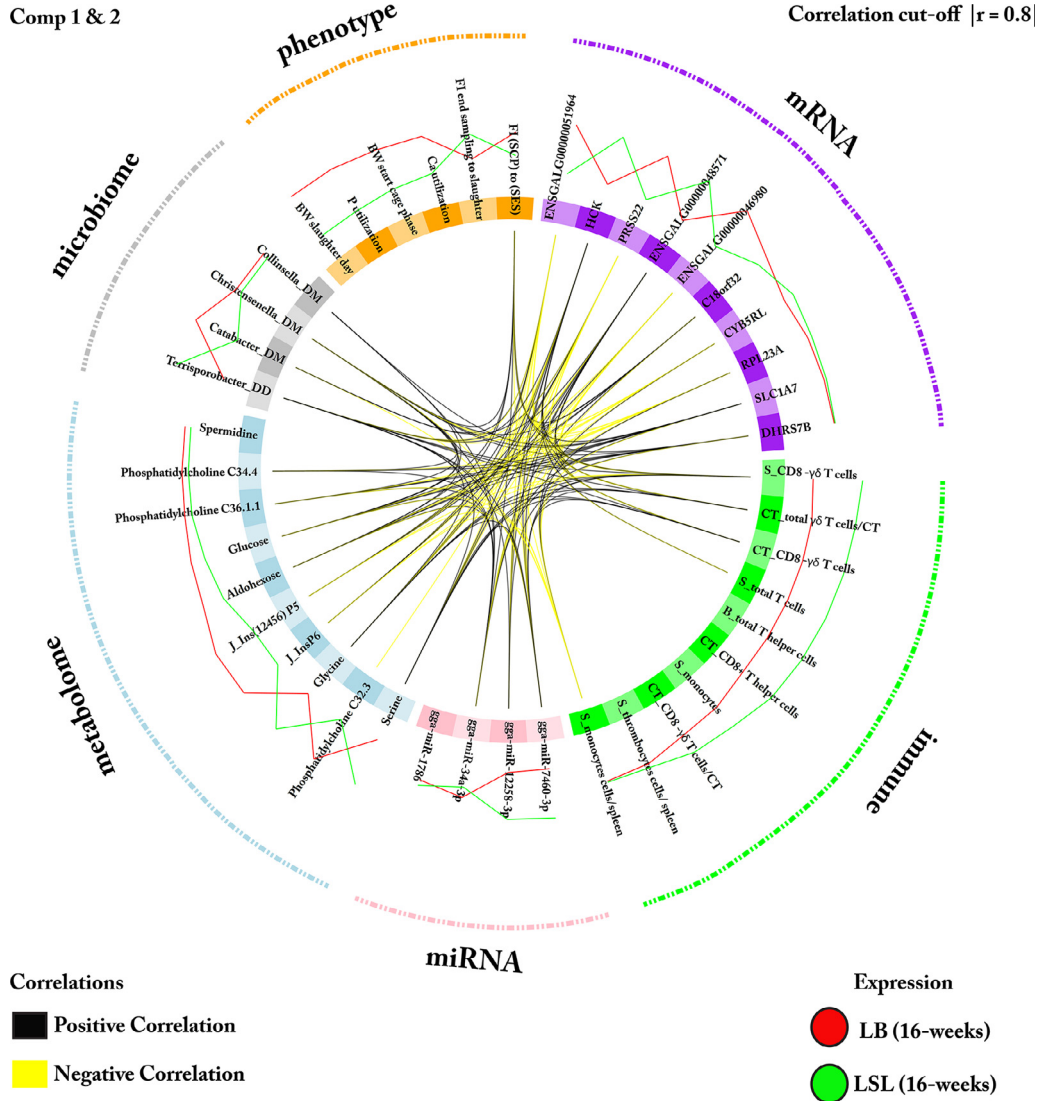


Figure 5. Circos plot indicating the significant biosignatures from multiple datasets based on the Pearson correlation coefficient $|r| = 0.8$ over the two components. The selected biomarkers were represented in the inner circle. Similarly to Figure 4, the purple, green, pink, blue, gray, orange dashed lines outside the circos indicate each data type. The black link suggests a positive correlation, while the yellow link depicts a negative correlation. The red and green lines represent the features' expression in LB and LSL at (wk-16), respectively.

unclassified Ruminococcaceae showed no enrichment in pathway analysis. Interestingly, intestinal transcripts correlating with *Anaerobiospirillum* were enriched in D-myo-inositol (1,4,5)-trisphosphate degradation ($P = 6.9 \times 10^{-6}$).

DISCUSSION

In this study, we describe the results of an integrated longitudinal multi-omics analysis of the gut microbiome, metabolome, host intestinal transcripts (mRNA and miRNA), immune cells, and other phenotypic traits of 2 laying hen strains along 5 production periods.

Abundances of molecular features of longitudinal changes and separate the pre-laying and egg-laying period for both strains. Transcripts from the phosphatidylethanolamine binding protein 1 (*PEBP1*) and V-set and immunoglobulin domain containing 10 (*VSIG10*) were strongly expressed in the intestine at the pre-laying

period. The intestine is a tissue with high cell turnover and a lifelong regenerative function of stem cells. *PEBP1* has been connected with the regenerative potential of intestinal stem cells, it is highly expressed in intestinal enterocytes, and downregulated with age and under oxidative stress (Pyo et al., 2018). *VSIG10* is involved in cell to cell adhesion, may relate to stem cell function, and has an unexamined role in colonic pathobiologies (Iftikhar et al., 2022). Similarly, miRNA-122-5p and miR-181b-5p were more abundant in the pre-laying period in both strains. These two miRNAs were previously found to be associated with inositol phosphate metabolism (Ponsuksili et al., 2021), cell proliferation (Yang et al., 2018), phosphatidylcholine, blood Ca, as well as lipid metabolism, including bile acid metabolism in hepatocytes and enterocytes (Ito and Adachi-Akahane, 2013).

Microbial taxa including *Fusobacterium*, *Lactococcus*, and *Veillonella* were more abundant in laying period with specific demands for egg production.

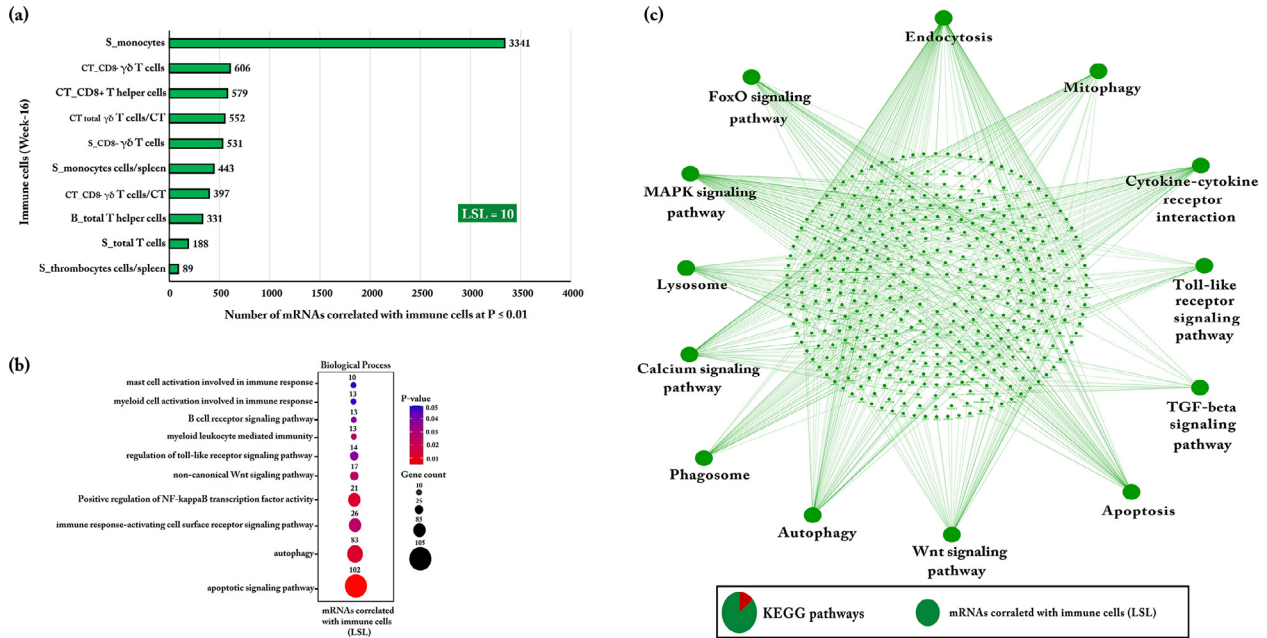


Figure 6. Gene Ontology and KEGG pathways enrichment analysis of mRNAs correlated with immune cell types within LB and LSL at wk 16. (A) The bar chart indicates the number of mRNAs correlated with immune cell types at $P \leq 0.01$ in LSL. The green bar shows the abundance of immune cell types in LSL, while no immune cell type was identified in LB. (B) Gene Ontology enrichment analyses (biological process) for transcripts correlated with immune cell types in LSL. The size of the dots represents the number of transcripts involved in each biological process, while the color indicates the significance. (C) KEGG pathway enrichment analysis of mRNAs correlated with immune cells in LSL. The pie charts indicate the strain-specific proportions of mRNAs correlated with immune cells to the KEGG pathways. The green ellipse depicts mRNAs correlated with immune cells in LSL. KEGG pathways and biological processes with $P \leq 0.05$ were considered significant.

Fusobacterium was identified as potential butyrate producer (Vital et al., 2014), while *Lactococcus* and *Veillonella* were reported to contribute to phytate degradation (Reyer et al., 2021) and digestion of

cellulose (Sun et al., 2016). Many studies have highlighted the importance of these microbiota-derived short-chain fatty acids (SCFAs) such as butyrate, which serves as primary energy sources in the gut and

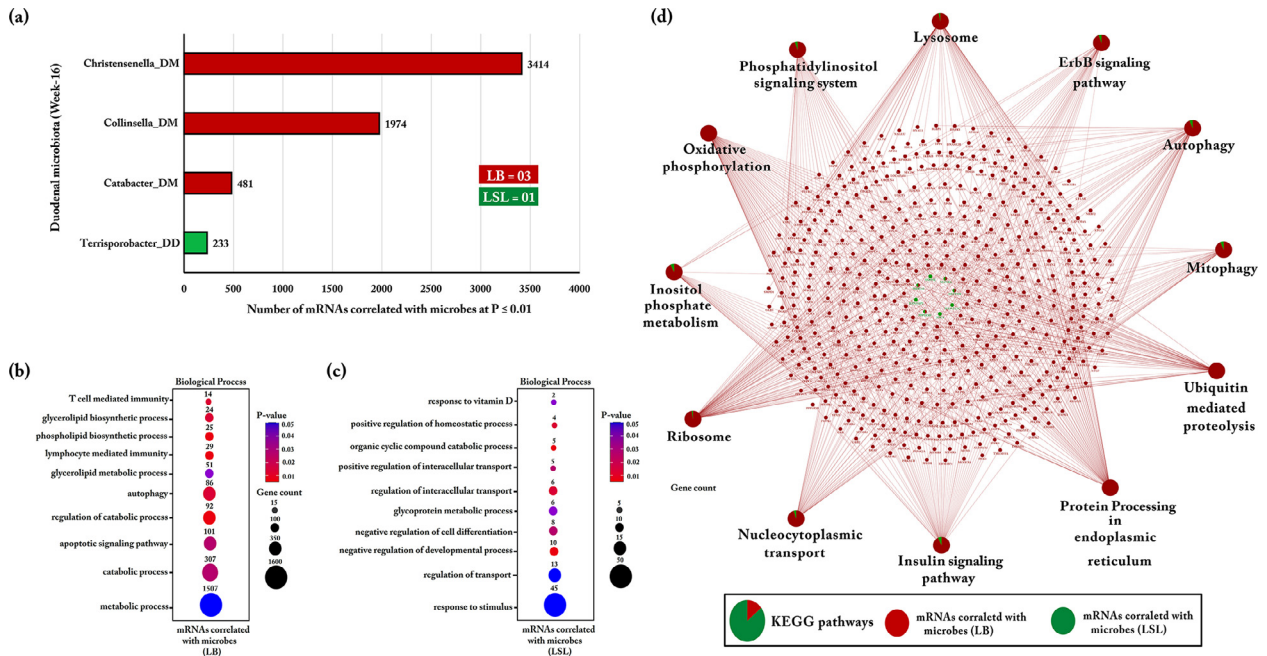


Figure 7. Gene Ontology and KEGG pathways enrichment analysis of mRNAs correlated with duodenal microbiota within LB and LSL at wk 16. (A) The bar chart indicates the number of mRNAs correlated with microbes at $P \leq 0.01$ within LB and LSL. The green bar shows more abundant microbes in LSL and the red bars depict more abundant microbes in LB. (B and C) Gene Ontology (biological processes) enrichment analysis for the transcripts correlated with microbes in LB and LSL, respectively. The size of the dots represents the number of transcripts involved in each biological process, while the color indicates the significance. (D) KEGG pathway enrichment analysis of mRNAs correlated with microbes within LB and LSL. The pie charts indicate the strain-specific proportions of mRNAs correlated with microbiota in the KEGG pathways. The red ellipse shows mRNAs correlated with microbes in LB, and the green ellipse depict mRNAs correlated with microbes in LSL. KEGG pathways and biological processes with $P \leq 0.05$ were considered significant.

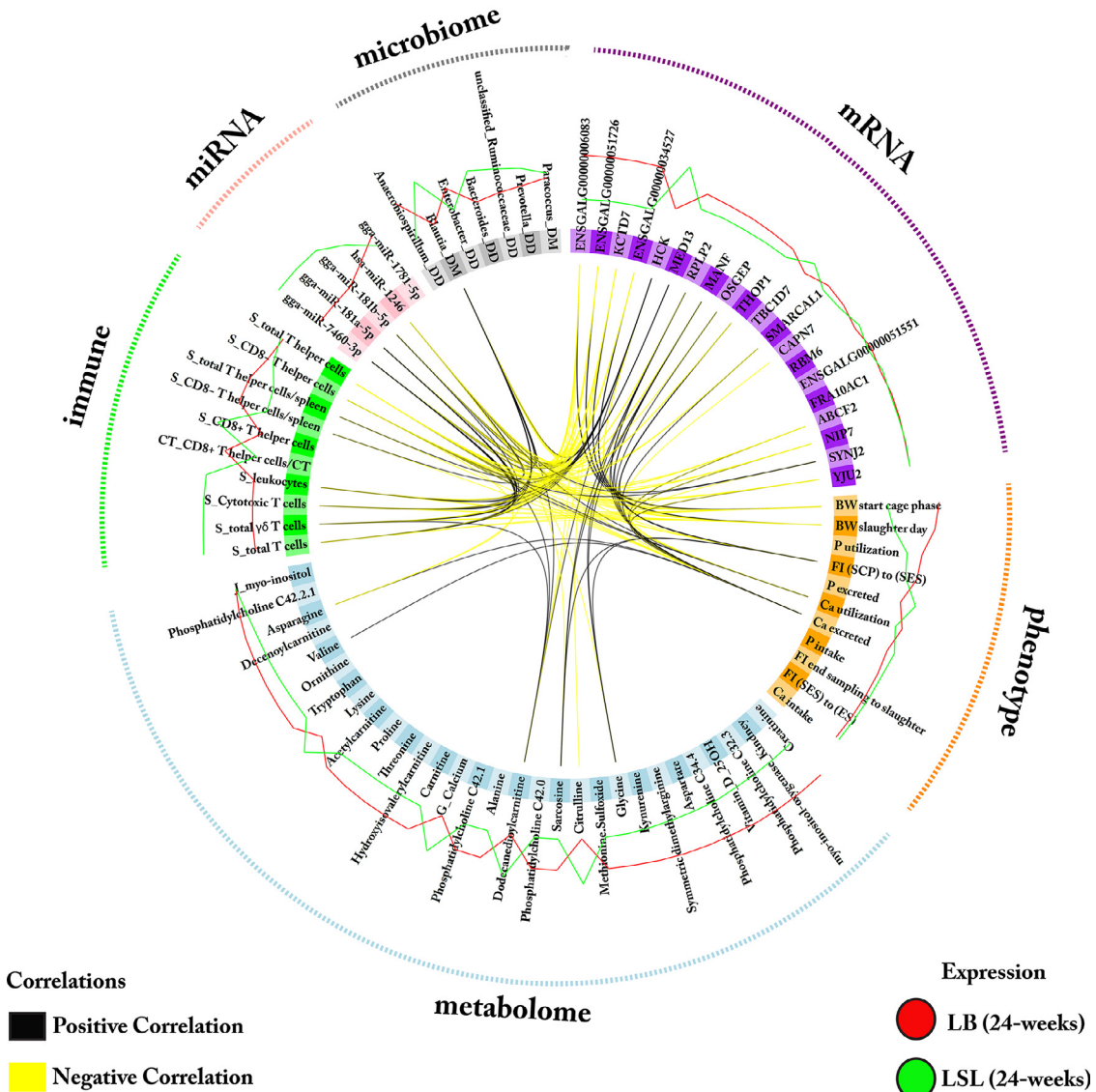


Figure 8. Circos plot indicating the significant biosignatures from multiple datasets. The plot shows Pearson correlation coefficients $|r| = 0.8$ over the two components. The selected biomarkers are represented in the inner circle. Similarly, the purple, orange, blue, green, pink, gray dashed lines outside the circos indicate each data type. The black link suggests a positive correlation, while the yellow link depicts a negative correlation. The red and green lines represent the feature expression in LB and LSL at (wk-24), respectively.

also acts as an immunomodulatory agent (LIT) (Qin et al., 2012; Karlsson et al., 2013). We found highly positive correlation between *Lactococcus*, *Veillonella*, and *Fusobacterium* and splenic immune cell counts that were elevated in the laying period. The knowledge how specific microbiota shift or modulate the immune system is still limited.

Among the selected features from the group of transcripts, those with higher abundance after onset of laying are steroidogenic acute regulatory protein-related lipid transfer 4 (*STARD4*), methylsterol monooxygenase 1 (*MSMO1*) and 3-hydroxy-3-methylglutaryl-CoA reductase (*HMGCR*). *STARD4* is an important cholesterol transporter involved in sterol sensing and maintaining lipid homeostasis (Iaea et al., 2020). *HMGCR* belonging to mevalonate pathway enzymes also plays a role in cholesterol synthesis and is the rate-limiting enzyme for cholesterol synthesis, mostly occurring in

liver. Many digestive enzymes can be secreted from the intestinal epithelial cells into the intestinal lumen to metabolize lipids. Therefore, transcripts related to lipid metabolism pathways were also observed in mammalian and fish small intestines (Tokuhara et al., 2014; Okamura et al., 2021). As shown here, *HMGCR* displays high expression after onset of laying, whereas miR-122, a microRNA also involved in lipid metabolism, was highly expressed in pre-laying phase. Hepatic knock-down of miR-122 significantly decreased serum triglyceride and total cholesterol levels (Lagos-Quintana et al., 2002). MiR-122 indirectly downregulated a set of genes involved in cholesterol biosynthesis, including *HMGCR* and *HMGCS1* (Esau et al., 2006). Consistent with other studies, this study showed that *HMGCR* and *HMGCS1* were downregulated even in the intestinal mucosa, whereas miR-122 was more pronounced in the prelaying phase and conversely after the onset of laying. Similarly

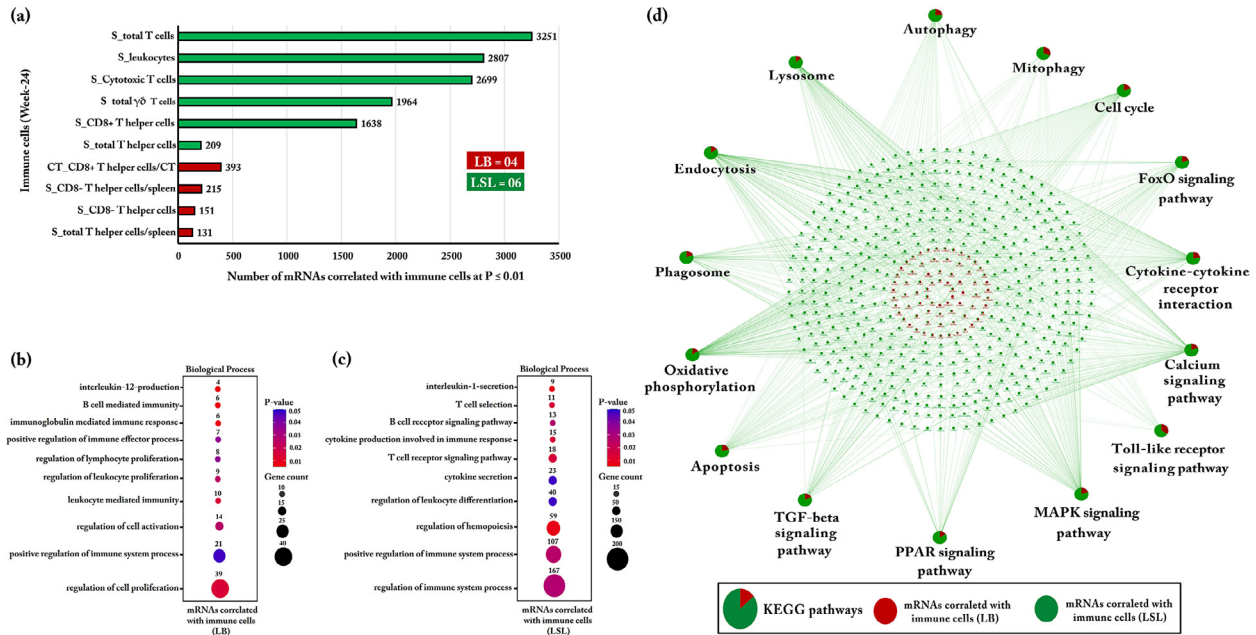


Figure 9. Gene Ontology and KEGG pathways enrichment analysis of mRNAs correlated with immune cell types for LB and LSL at wk 24. (A) The bar chart plot shows the number of mRNAs correlated with immune cell types at a significance level of $P \leq 0.01$ for LB and LSL. The green bars show abundant immune cell types in LSL and the red bars indicate abundant immune cell types in LB. (B and C) Gene Ontology (biological processes) enrichment analysis for the transcripts correlated with immune cell types in LB and LSL, respectively. The size of the dots represents the number of transcripts involved in each biological process, while the color indicates its significance. (D) KEGG pathway enrichment analysis of mRNAs correlated with microbes for LB and LSL. The pie charts indicate the strain-specific proportions of mRNAs correlated with microbiota in the KEGG pathways. The red ellipse shows mRNAs correlated with immune cell types in LB, and the green ellipse depict mRNAs correlated with immune cell types in LSL. KEGG pathways and biological processes with $P \leq 0.05$ were considered significant.

to *STARD4* and *HMGCR*, *MSMO1* is also involved in cholesterol biosynthetic process. All this evidence suggests that lipid metabolism in the intestine is important

during the laying period. The shifts in abundances of transcripts, microbiota, and metabolites from the pre-laying period to the laying period may relate to the

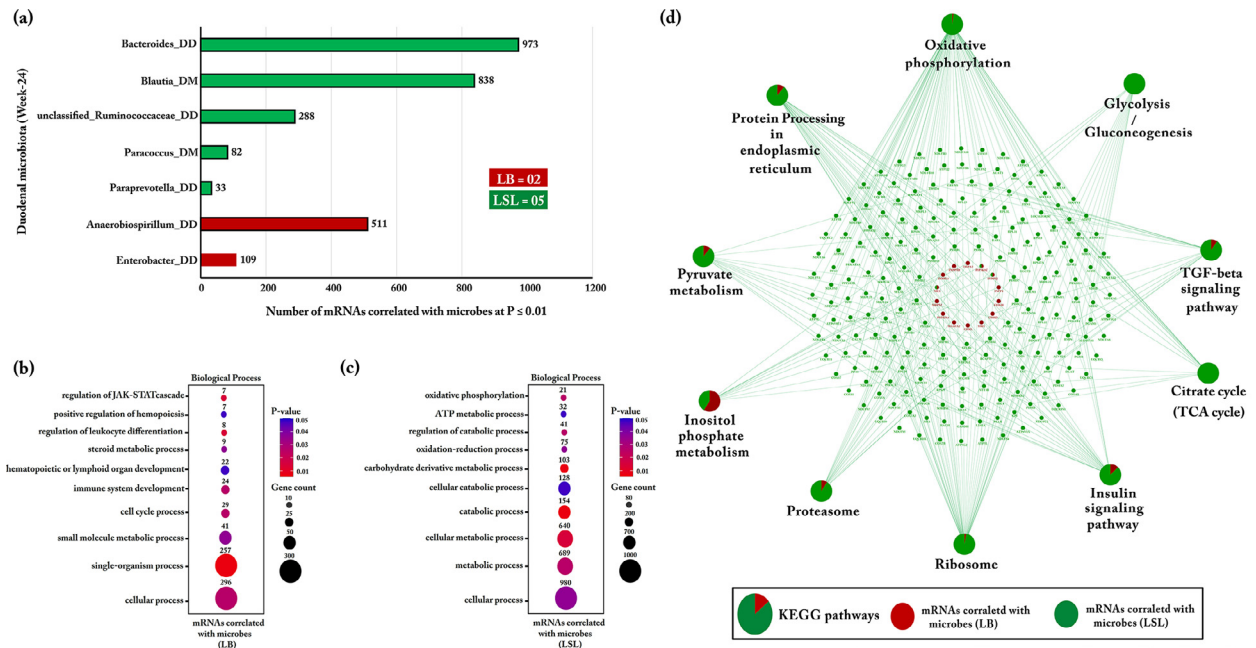


Figure 10. Gene Ontology and KEGG pathways enrichment analysis of mRNAs correlated with duodenal microbiota within LB and LSL at wk 24. (A) The bar chart indicates the number of mRNAs correlated with microbes at a significance of $P \leq 0.01$ for LB and LSL. The green bars show more abundant microbes in LSL and the red bars depict more abundant microbes in LB. (B and C) Gene Ontology (biological processes) enrichment analysis for the transcripts correlated with immune cell types in LB and LSL, respectively. The size of the dots represents the number of transcripts involved in each biological process, while the color indicates its significance. (D) KEGG pathway enrichment analysis of mRNAs correlated with microbes within LB and LSL. The pie charts indicate the strain-specific proportions of mRNAs correlated with microbiota to the KEGG pathways. The red ellipse shows mRNAs correlated with microbes in LB and the green ellipse depict mRNAs correlated with microbes in LSL. KEGG pathways and biological processes with $P \leq 0.05$ were considered significant.

metabolic and nutritional requirements exerted by the production of eggs in both strains.

Several of the selected features that differentiate across the chicken life cycle showed peak expression levels at 24 wk, including microbes assigned to *Enhydrobacter* and *Mycoplasma*, as well as several mRNA and miRNA transcripts. Phospholipase A2 group VI (*PLA2G6*) was one of the biosignatures for the onset of egg laying. *PLA2G6* expression was more pronounced during the laying period and it was weakened after 30 wk. Deficiency of *PLA2G6* caused a decline in important homeostatic genes in the intestine, leading to the development of gastrointestinal diseases and sensitizing to gastrointestinal damage with age (Jiao et al., 2017). *IRF1*, which involves the biosynthesis of interleukin-12 production, was found to be also part of this profile. Microbial stimulation enables IRF8 to associate with other transcription factors, including IRF1, to induce immune response genes (Mancino et al., 2015). IRF1 was also reported as a potential gene regulatory factor of *Irfl* gene in bone metabolism (Salem et al., 2014).

While immune cells, especially from the blood, were predominantly present in the period before laying, the immune cells from the spleen and cecal tonsil were dominant in the period of laying. Egg-laying activity seems to alter the immune system toward a more pronounced humoral and innate immune response (Schmucker et al., 2021). In laying hens, particularly during laying activity, infectious diseases were shown to account for up to 12% of deaths (Herwig et al., 2021). The laying period, as a stress period in laying hen, is accompanied by shifts in immune cells, immune pathways, and interactions with particular gut microbiota, for instance, *Enhydrobacter* and *Mycoplasma*. These two genera exhibited highly abundance at 24 wk. Although many species of *Mycoplasma* can infect laying hens, only *Mycoplasma gallisepticum* and *Mycoplasma synoviae* are pathogenic for chickens. In our study, *Mycoplasma penetrans* was identified. Integration of microbiota, immune and transcripts data confirmed that innate immune response cell along with interleukin-12 production transcript and microbiota composition dominated in the laying phase.

Further we identified omics-biosignatures consist of 40 mRNAs, 14 miRNAs, 15 microbial taxa, 30 metabolites, 45 immune traits, and 15 other phenotype traits derived from three component sets per age group and per strain. Transcripts of metabolic pathways were strong biosignatures for discrimination of production period and strain including *AKR1E2*, *HMGCR*, *IVD*, *MSMO1*, *MTHFS*, *PAPSS2*, and *ST6GALNAC1*. Biosynthesis of interleukin-12 production (*IRF1*) and IL-15 production (*IRF1* and *HCK*) were also identified as biosignatures. Hematopoietic cell kinase (*HCK*), a member of the Src family of non-receptor tyrosine kinases (*NRTKs*), is mainly expressed in myeloid cells and highly expressed in macrophages during macrophage activation. *HCK* is involved in various inflammatory responses (English et al., 1993). Interestingly, this transcript was highly expressed in LSL at all stages compared to LB strain. Consistent with our previous study, miRNAs are

part of the biosignature targeting transcripts related to pathways of energy metabolism (mmu-miR-6240, gga-miR-12258-3p, and gga-miR-2131-3p) and inositol phosphate metabolism (miR-181b-5p, miR-122-5p, and miR-1454).

Focussing on differences between wk 16 and 24, associated with most prominent physiological changes due to the onset of laying, in both strains we found that the features such as *HCK*, CD8⁻ $\gamma\delta$ T cells, total T cells, miR-7460-3p, miR-181a-5p, *Terrisporobacter*, *Blautia*, and serine in serum were more abundant in LSL than LB. The role of *Blautia* in inflammatory and metabolic diseases and its probiotic properties have been previously reviewed (Liu et al., 2021). We also found gut transcripts that negatively correlated with *Blautia* were enriched in metabolic and energy metabolism pathways. Therefore, the greater abundance of *Blautia* in LSL might be related to the greater abundance of immune cells, the higher defensiveness and the reduced metabolic process of LSL. This association implies the strong host-gut interaction in the LSL strain. The study previously conducted on the same birds, looking only at immune cells, also confirms that certain life stages were associated with changes in the number and function of immune cells in LB and LSL hens (Schmucker et al., 2021). In this context, the innate and humoral immune response is more pronounced in LB hens, while the cellular arm of the immune system is more pronounced in LSL hens (Hofmann et al., 2021; Schmucker et al., 2021). Previous studies have shown that interactions between gut microbiota and host stimulate the host immune system (Thaiss et al., 2016).

Our previous study reported that miRNAs, including miR-181b-5p, miR-99a-5p, miR-145-5p, miR-122-5p, let-7b, miR-143-3p, miR-21, and miR-221-3p, modulate the expression of host genes enriched in inositol phosphate metabolism and immune signaling pathways, with the most pronounced changes at 16 to 24 wk of age (Ponsuksili et al., 2021). Phytate (inositol hexakisphosphate) is a form of phosphate storage in plant seeds and is thus present in laying hen diets. Microbial phytase contributes to the intestinal degradation of inositol phosphates, simultaneously releasing P and lower inositol phosphates (Stentz et al., 2014). Microbiota-derived inositol phosphate, InsP₃, was shown to regulate the histone deacetylase 3 (HDAC3) activity promoting epigenetic changes and epithelial repair in the host intestine (Wu et al., 2020). Interestingly, we found a number of histone deacetylase, differently expressed between 16 wk compared to 24 wk (FDR <5%) in both strains. *HDAC3* was downregulated in LSL compared to LB strain at 24 wk (FDR <5%). Interestingly, the correlation of host transcripts with the microbiota of the LB indicated enrichment for inositol phosphate metabolism at both wk 16 and 24. The LB strain, which is particularly prominent in the metabolic pathways during the laying periods, underwent a development of symbiotic host-microbiota relationships due to its beneficial commensal microbiota. In contrast, the immune system played a prominent role in the LSL strain, as evidenced by the

abundant immune cells in many organs such as blood, spleen, and cecal tonsils. This recent integration of omics data confirms that LB and LSL strains employ different inherent strategies to acquire and maintain their immune and metabolic systems under high-performance conditions (Iqbal et al., 2022).

The onset of the laying period is also characterized by changes in a number of traits specific to each of the 2 strains. These findings confirm that in LB and LSL, differences in body weight and feed intake and utilization, are associated with further changes in molecular traits, such as abundances of metabolites and transcripts related to energy metabolic pathways, as well as the immune system and microbiota that occur at this critical period (Sommerfeld et al., 2020a, 2020b; Omotoso et al., 2021; Ponsuksili et al., 2021).

The mechanistic, bioinformatic integration of data from different biological levels provides biosignatures specific to the strains and production time points considered, consisting of biomarkers that are key in terms of best discrimination. A number of them are also indicative in terms of molecular pathways taken differently in the 2 strains. The study confirms the previously shown differences between the strains in terms of the activity of immunological and metabolic functions and pathways, highlighting in particular that interaction between host and gut microbiota play an important role in immune response and metabolic homeostasis at different genetic backgrounds and in different production periods. However, the reduction in data dimension and fragmentation of data at different biological levels complicate the automatic functional annotation of biosignature features and do not absolve the need to manually inspect specific pathways.

ACKNOWLEDGMENTS

This work was financially supported by the Deutsche Forschungsgemeinschaft (DFG, German Research Foundation) – Project number WI 3719/8-1, WI 1754/16-1, CA 1708/2-1 and RO 1217/10-1 as part of the research unit P-FOWL (FOR 2601). The authors thank Nicole Gentz, Annette Jugert, and Joana Bittner for excellent technical assistance for their help in preparing the samples, RNA extraction and sequencing.

DISCLOSURES

All authors declare no conflicts of interests.

SUPPLEMENTARY MATERIALS

Supplementary material associated with this article can be found in the online version at [doi:10.1016/j.psj.2022.102256](https://doi.org/10.1016/j.psj.2022.102256).

REFERENCES

- Barko, P. C., M. A. McMichael, K. S. Swanson, and D. A. Williams. 2018. The gastrointestinal microbiome: a review. *J. Vet. Intern. Med.* 32:9–25.
- Bindea, G., J. Galon, and B. Mlecnik. 2013. CluePedia Cytoscape plugin: pathway insights using integrated experimental and in silico data. *Bioinformatics* 29:661–663.
- Bindea, G., B. Mlecnik, H. Hackl, P. Charoentong, M. Tosolini, A. Kirilovsky, W. H. Fridman, F. Pagès, Z. Trajanoski, and J. Galon. 2009. ClueGO: a Cytoscape plug-in to decipher functionally grouped gene ontology and pathway annotation networks. *Bioinformatics* 25:1091–1093.
- Borda-Molina, D., M. Vital, V. Sommerfeld, M. Rodehutschord, and A. Camarinha-Silva. 2016. Insights into broilers' gut microbiota fed with phosphorus, calcium, and phytase supplemented diets. *Front. Microbiol.* 7:2033.
- Chong, J., O. Soufan, C. Li, I. Caraus, S. Li, G. Bourque, D. S. Wishart, and J. Xia. 2018. MetaboAnalyst 4.0: towards more transparent and integrative metabolomics analysis. *Nucl. Acids. Res.* 46:W486–W494.
- English, B. K., J. N. Ihle, A. Myracle, and T. Yi. 1993. Hck tyrosine kinase activity modulates tumor necrosis factor production by murine macrophages. *J. Exp. Med.* 178:1017–1022.
- Esau, C., S. Davis, S. F. Murray, X. X. Yu, S. K. Pandey, M. Pear, L. Watts, S. L. Booten, M. Graham, R. McKay, A. Subramaniam, S. Propp, B. A. Lollo, S. Freier, C. F. Bennett, S. Bhanot, and B. P. Monia. 2006. miR-122 regulation of lipid metabolism revealed by in vivo antisense targeting. *Cell Metab.* 3:87–98.
- Gonzalez-Uarquin, F., V. Sommerfeld, M. Rodehutschord, and K. Huber. 2021. Interrelationship of myo-inositol pathways with systemic metabolic conditions in two strains of high-performance laying hens during their productive life span. *Sci. Rep.* 11:4641.
- Habig, C., R. Geffers, and O. Distl. 2012. Differential gene expression from genome-wide microarray analyses distinguishes lohmann selected leghorn and lohmann brown layers. *PLoS One* 7:e46787.
- Heinritz, S. N., E. Weiss, M. Eklund, T. Aumiller, S. Louis, A. Rings, S. Messner, A. Camarinha-Silva, J. Seifert, S. C. Bischoff, and R. Mosenthin. 2016. Intestinal microbiota and microbial metabolites are changed in a pig model fed a high-fat/low-fiber or a low-fat/high-fiber diet. *PLoS One* 11:e0154329.
- Herwig, E., C. L. Walk, M. Bedford, K. Schwean-Lardner, and H. L. Classen. 2021. Contrasting the effects of phytase and pure myo-inositol on the performance, digestibility, blood and egg yolk inositol levels and digestion physiology of laying hens. *Br. Poult. Sci.* 62:517–527.
- Hofmann, T., S. Schmucker, V. Sommerfeld, K. Huber, M. Rodehutschord, and V. Stefanski. 2021. Immunomodulatory effects of dietary phosphorus and calcium in two strains of laying hens. *Animals* 11:129.
- Iaea, D. B., Z. R. Spahr, R. K. Singh, R. B. Chan, B. Zhou, R. Bareja, O. Elemento, G. Di Paolo, X. Zhang, and F. R. Maxfield. 2020. Stable reduction of STARD4 alters cholesterol regulation and lipid homeostasis. *Biochimica et biophysica acta. Mol. Cell Biol. Lipids* 1865:158609.
- Iftikhar, R., H. M. Penrose, A. N. King, Y. Kim, E. Ruiz, E. Kandil, H. L. Machado, and S. D. Savkovic. 2022. FOXO3 expression in macrophages is lowered by a high-fat diet and regulates colonic inflammation and tumorigenesis. *Metabolites* 12:250.
- Iqbal, M. A., H. Reyer, M. Oster, F. Hadlich, N. Trakooljul, A. Perdomo-Sabogal, S. Schmucker, V. Stefanski, C. Roth, A. Camarinha Silva, K. Huber, V. Sommerfeld, M. Rodehutschord, K. Wimmers, and S. Ponsuksili. 2022. Multi-omics reveals different strategies in the immune and metabolic systems of high-yielding strains of laying hens. *Front. Genet.* 13:858232.
- Ito, M., and S. Adachi-Akahane. 2013. Inter-organ communication in the regulation of lipid metabolism: focusing on the network between the liver, intestine, and heart. *J. Pharmacol. Sci.* 123:312–317.
- Jiao, L., H. Gan-Schreier, X. Zhu, W. Wei, S. Tuma-Kellner, G. Liebisch, W. Stremmel, and W. Chamulitrat. 2017. Ageing sensitized by iPLA(2) β deficiency induces liver fibrosis and intestinal atrophy involving suppression of homeostatic genes and alteration of intestinal lipids and bile acids. *Biochimica et biophysica acta. Mol. Cell Biol. Lipids.* 1862:1520–1533.

- Karlsson, F. H., V. Tremaroli, I. Nookaew, G. Bergström, C. J. Behre, B. Fagerberg, J. Nielsen, and F. Bäckhed. 2013. Gut metagenome in European women with normal, impaired and diabetic glucose control. *Nature* 498:99–103.
- Kaufmann, F., G. Daş, R. Preisinger, M. Schmutz, S. König, and M. Gauly. 2011. Genetic resistance to natural helminth infections in two chicken layer lines. *Vet. Parasitol.* 176:250–257.
- Lagos-Quintana, M., R. Rauhut, A. Yalcin, J. Meyer, W. Lendeckel, and T. Tuschl. 2002. Identification of tissue-specific microRNAs from mouse. *Curr. Biol.* CB 12:735–739.
- Liu, X., B. Mao, J. Gu, J. Wu, S. Cui, G. Wang, J. Zhao, H. Zhang, and W. Chen. 2021. Blautia-a new functional genus with potential probiotic properties? *Gut. Microbes.* 13:1–21.
- Love, M. I., W. Huber, and S. Anders. 2014. Moderated estimation of fold change and dispersion for RNA-seq data with DESeq2. *Genome Biol.* 15:550.
- Mancino, A., A. Termanini, I. Barozzi, S. Ghisletti, R. Ostuni, E. Prosperini, K. Ozato, and G. Natoli. 2015. A dual cis-regulatory code links IRF8 to constitutive and inducible gene expression in macrophages. *Genes Dev* 29:394–408.
- Okamura, Y., H. Miyanishi, M. Kinoshita, T. Kono, M. Sakai, and J. I. Hikima. 2021. A defective interleukin-17 receptor A1 causes weight loss and intestinal metabolism-related gene downregulation in Japanese medaka, *Oryzias latipes*. *Sci. Rep.* 11:12099.
- Omotoso, A. O., H. Reyer, M. Oster, S. Ponsuksili, N. Trakooljul, E. Muráni, V. Sommerfeld, M. Rodehutsord, and K. Wimmers. 2021. Jejunal transcriptomic profiling of two layer strains throughout the entire production period. *Sci. Rep.* 11:20086.
- Ottman, N., H. Smidt, W. M. de Vos, and C. Belzer. 2012. The function of our microbiota: who is out there and what do they do? *Front. Cell Infect. Microbiol.* 2:104.
- Ponsuksili, S., F. Hadlich, H. Reyer, M. Oster, N. Trakooljul, M. A. Iqbal, V. Sommerfeld, M. Rodehutsord, and K. Wimmers. 2021. Genetic background and production periods shape the microRNA profiles of the gut in laying hens. *Genomics* 113:1790–1801.
- Pyo, J. H., H. J. Jeon, J. S. Park, J. S. Lee, H. Y. Chung, and M. A. Yoo. 2018. Drosophila PEBP1 inhibits intestinal stem cell aging via suppression of ERK pathway. *Oncotarget* 9:17980–17993.
- Qin, J., Y. Li, Z. Cai, S. Li, J. Zhu, F. Zhang, S. Liang, W. Zhang, Y. Guan, D. Shen, Y. Peng, D. Zhang, Z. Jie, W. Wu, Y. Qin, W. Xue, J. Li, L. Han, D. Lu, P. Wu, Y. Dai, X. Sun, Z. Li, A. Tang, S. Zhong, X. Li, W. Chen, R. Xu, M. Wang, Q. Feng, M. Gong, J. Yu, Y. Zhang, M. Zhang, T. Hansen, G. Sanchez, J. Raes, G. Falony, S. Okuda, M. Almeida, E. LeChatelier, P. Renault, N. Pons, J. M. Batto, Z. Zhang, H. Chen, R. Yang, W. Zheng, S. Li, H. Yang, J. Wang, S. D. Ehrlich, R. Nielsen, O. Pedersen, K. Kristiansen, and J. Wang. 2012. A metagenome-wide association study of gut microbiota in type 2 diabetes. *Nature* 490:55–60.
- Reyer, H., P. J. R. Sjöberg, M. Oster, A. Wubuli, E. Murani, S. Ponsuksili, P. Wolf, and K. Wimmers. 2021. Mineral phosphorus supply in piglets impacts the microbial composition and phytate utilization in the large intestine. *Microorganisms* 9:1197.
- Rodehutsord, M. 2017. Advances in understanding the role of phytate in phosphorus and calcium nutrition of poultry. Pages 165–180 in *Achieving Sustainable Production of Poultry Meat. Breeding and Nutrition* (ed. T. Applegate) Burleigh Dodds, Cambridge, UK Volume 2.
- Rohart, F., B. Gautier, A. Singh, and K. A. Lê Cao. 2017. mixOmics: an R package for “omics feature selection and multiple data integration. *PLoS Comput. Biol.* 13:e1005752.
- Salem, S., C. Gao, A. Li, H. Wang, L. Nguyen-Yamamoto, D. Goltzman, J. E. Henderson, and P. Gros. 2014. A novel role for interferon regulatory factor 1 (IRF1) in regulation of bone metabolism. *J. Cell Mol. Med.* 18:1588–1598.
- Schmucker, S., T. Hofmann, V. Sommerfeld, K. Huber, M. Rodehutsord, and V. Stefanski. 2021. Immune parameters in two different laying hen strains during five production periods. *Poult. Sci.* 100:101408.
- Singh, A., C. P. Shannon, B. Gautier, F. Rohart, M. Vacher, S. J. Tebbutt, and L. C. KA. 2019a. DIABLO: an integrative approach for identifying key molecular drivers from multi-omics assays. *Bioinformatics* 35:3055–3062.
- Singh, A., C. P. Shannon, B. Gautier, F. Rohart, M. Vacher, S. J. Tebbutt, and K. A. Lê Cao. 2019b. DIABLO: an integrative approach for identifying key molecular drivers from multi-omics assays. *Bioinformatics* 35:3055–3062.
- Sommerfeld, V., K. Huber, J. Jörn Bennewitz, A. Camarinha-Silva, M. Hasselmann, S. Ponsuksili, J. Seifert, V. Stefanski, K. Wimmers, and M. Rodehutsord. 2020a. Phytate degradation, myo-inositol release, and utilization of phosphorus and calcium by two strains of laying hens in five production periods. *Poult. Sci.* 99:6797–6808.
- Sommerfeld, V., A. O. Omotoso, M. Oster, H. Reyer, A. Camarinha-Silva, M. Hasselmann, K. Huber, S. Ponsuksili, J. Seifert, V. Stefanski, K. Wimmers, and M. Rodehutsord. 2020b. phytate degradation, transcellular mineral transporters, and mineral utilization by two strains of laying hens as affected by dietary phosphorus and calcium animals 10:1736.
- Stentz, R., S. Osborne, N. Horn, A. W. Li, I. Hautefort, R. Bongaerts, M. Rouyer, P. Bailey, S. B. Shears, A. M. Hemmings, C. A. Brearley, and S. R. Carding. 2014. A bacterial homolog of a eukaryotic inositol phosphate signaling enzyme mediates cross-kingdom dialog in the mammalian gut. *Cell Rep.* 6:646–656.
- Sun, B., X. Wang, S. Bernstein, M. A. Huffman, D. P. Xia, Z. Gu, R. Chen, L. K. Sheeran, R. S. Wagner, and J. Li. 2016. Marked variation between winter and spring gut microbiota in free-ranging Tibetan Macaques (*Macaca thibetana*). *Sci. Rep.* 6:26035.
- Thaiss, C. A., N. Zmora, M. Levy, and E. Elinav. 2016. The microbiome and innate immunity. *Nature* 535:65–74.
- Tokuhara, D., T. Nochi, A. Matsumura, M. Mejima, Y. Takahashi, S. Kurokawa, H. Kiyono, and Y. Yuki. 2014. Specific expression of apolipoprotein A-IV in the follicle-associated epithelium of the small intestine. *Dig. Dis. Sci.* 59:2682–2692.
- Vital, M., A. C. Howe, and J. M. Tiedje. 2014. Revealing the bacterial butyrate synthesis pathways by analyzing (meta)genomic data. *mBio* 5:e00889.
- Wu, S. E., S. Hashimoto-Hill, V. Woo, E. M. Eshleman, J. Whitt, L. Engleman, R. Karns, L. A. Denson, D. B. Haslam, and T. Alenghat. 2020. Microbiota-derived metabolite promotes HDAC3 activity in the gut. *Nature* 586:108–112.
- Yang, M., X. Zhai, T. Ge, C. Yang, and G. Lou. 2018. miR-181a-5p promotes proliferation and invasion and inhibits apoptosis of cervical cancer cells via regulating inositol polyphosphate-5-phosphatase A (INPP5A). *Oncol Res* 26:703–712.